Analysis of Electromagnetic Characteristics of a Grounded Slab and a Parallel-Plate Structure Using the SDDI Technique

Jaehoon Choi and Sungtek Kahng

In this paper, the electromagnetic characteristics of a grounded slab and a parallel-plate structure are analyzed by the Spline-type Divided-Difference Interpolation (SDDI) technique. The technique efficiently evaluates the MoM impedance matrix elements of the multifold spectral or spatial domain integrals or summation in integrodifferential equations. The numerical results of the proposed method agree well with those of the corresponding literatures.

Manuscript received May 16, 2000; revised May 4, 2001.
Jaehoon Choi is with the Hanyang University, Seoul, Korea.
(phone: +82 2 2290 0376, e-mail: choijh@hanyang.ac.kr)
Sungtek Kahng is with the Radio&Broadcasting Tech. Lab, ETRI, Taejon, Korea.
(phone: +82 42 860 6231, e-mail: s-kahng@etri.re.kr)

I. INTRODUCTION

When layered media problems are solved by the method of moment (MoM), the computational time is mainly determined by the spectral integration or summation of Green's functions or impedance matrix elements unless they are expressed as closed-forms [1], [2]. A number of researchers have tried to improve the numerical efficiency of evaluating spectral integrals [3], [4] or summation [5]. Fast computation of the Sommerfeld–type integrals has been combined with parabolic Lagrange interpolation [6]. Recently, the spectral integrals for Green's functions are decomposed into the fast converging terms and their asymptotic closed-forms [7]. Furthermore, combined with the technique in [7], the SDDI scheme is devised to more efficiently characterize RF devices [8]. In [8], spectral integration is performed using the SDDI.

Not as in [8], in this paper, the SDDI technique is used for solving integrodifferential equations including differentiation with respect to spatial variables. Spatial derivatives as well as integrals can be conveniently evaluated with the help of the spline concept and converging order of terms in divided-difference polynomials. Besides, the derivatives can be continuous in the spatial interval.

In Section II, the representative equations in the aforementioned case are established and the SDDI technique is briefly introduced. In Section III, electromagnetic radiation and scattering problems are analyzed using the SDDI technique. Though it can be applied to more complex structures, the electromagnetic characteristics of planar-layered media such as a microstrip patch, a line-fed microstrip patch antenna and a parallel plate

are analyzed via the SDDI technique in this paper. Finally, the numerical efficiency and accuracy of the proposed approach are compared to those of the corresponding references.

II. THEORY

1. Formulation

A. Spectral Domain Equation

The basis-expanded and tested dyadic Green's function of the spectral integral, which is often encountered in the evaluation of impedance matrix elements for the field equations, is given by

$$Z_{ij}(\vec{\rho}_m - \vec{\rho}_{sn}) = \frac{1}{4\pi^2}\int_{-\infty}^{+\infty}\int_{-\infty}^{+\infty} \widetilde{J}_{im}(k_i,k_j)\,\widetilde{G}_{ij}(k_i,k_j)\,\widetilde{J}_{jn}{}^{*}(k_i,k_j)\,dk_i dk_j \quad (1)$$

where $\widetilde{J}_{im}(k_i,k_j)$ and $\widetilde{G}_{ij}(k_i,k_j)$ are current density and a Green's function in the spectral domain, respectively. In (1), the subscripts i and j represent x, y or z, and $\vec{\rho}_m$ and $\vec{\rho}_{sn}$ stand for the m-th field and n-th source points, respectively.

B. Spatial Domain Equation

In analyzing the electromagnetic coupling problem, potentials need to be computed as usual. Particularly, when the external field penetrates through an aperture of a parallel plate waveguide, the boundary condition for the magnetic fields on the aperture is given by

$$\overline{H}^{s,-} + \overline{H}^{i,-} + \overline{H}^{r,-} = \overline{H}^{s,+}. \quad (2)$$

Superscripts + and - refer to the internal and external regions of the structure, respectively. $\overline{H}^{i}$, $\overline{H}^{r}$ and $\overline{H}^{s}$ stand for incident, reflected and scattered fields. The scattered magnetic field inside the parallel plate can be expressed as

$$\overline{H}^{s,+} = -j\frac{k_+}{\eta_+}\overline{F}^{+}(\bar{r}) - \nabla\phi_m{}^{+}(\bar{r}) \quad (3)$$

where $k_+ = \sqrt{\varepsilon_r\varepsilon_0\mu_0}$, $\eta_+ = \sqrt{\mu_0/\varepsilon_r\varepsilon_0}$ and ε_r is the relative permittivity inside the parallel plate. $\overline{F}^{+}(\bar{r}) = \int \overline{\overline{g}}^{+}{}_{m'n'}(\bar{r},\bar{r}')\cdot\overline{M}^{+}{}_{s}(\bar{r}')d\bar{r}'$ is electric vector potential, $\overline{\overline{g}}^{+}{}_{m'n'}(\bar{r},\bar{r}')$ is the Green's function, $\overline{M}^{+}{}_{s}$ is the magnetic current density, and m' and n' mean the directions of the vector potential and magnetic point source. $\phi_m{}^{+}(\bar{r})$ is the scalar potential, which is given by $\phi_m{}^{+}(\bar{r}) = j\frac{C}{k}\nabla\cdot\overline{F}^{+}(\bar{r})$. ∇ is del operator with respect to the observation coordinates, and C is the velocity of light. $\overline{\overline{g}}^{+}{}_{m'n'}(\bar{r},\bar{r}')$ is represented as

$$\overline{\overline{g}}^{+}{}_{m'n'}(\bar{r},\bar{r}') = \hat{m}'\hat{n}'\sum_{p=-\infty}^{+\infty}\frac{e^{-jk_+\sqrt{(x-x')^2+(y-y')^2+(z-z'+2pw)^2}}}{4\pi\sqrt{(x-x')^2+(y-y')^2+(z-z'+2pw)^2}} \quad (4)$$

where p denotes the integer and w is the separation of the two plates.

2. SDDI Technique

Since the SDDI is the extended version of the Divided-Difference Interpolation (DDI) [9], we briefly compare the DDI with the Lagrange Interpolation (LI) which is frequently adopted in numerical calculation. The numerical scheme of LI [9] is expressed as

$$P_n(R) = \sum_{p=0}^{n} f(R_p)\frac{l_p(R)}{l_p(R_p)}, \quad (5)$$

where

$$l_0(R) = (R-R_1)(R-R_2)\cdots(R-R_n)$$

$$l_p(R) = (R-R_0)\cdots(R-R_{p-1})(R-R_{p+1})\cdots(R-R_n)$$

$$(0 < p < n)$$

$$l_n(R) = (R-R_0)(R-R_1)\cdots(R-R_{n-1}).$$

$P_n(R)$, R_p, and $f(R_p)$ are the interpolating polynomial of order n, the p-th sampling point, and the value of an interpolated function at R_p, respectively. Whereas, the DDI scheme is given by

$$P_n(R) = f_0^{[0]} + Q_1(R) + Q_2(R) + \cdots + Q_v(R) + \cdots + Q_n(R) \quad (6)$$

where

$$Q_v(R) = (R-R_0)(R-R_1)\cdots(R-R_{v-1})f_0^{[v]}$$

$$f_u^{[v]} = f[R_u, R_{u+1}, \cdots, R_{u+v}] = \frac{f_{u+1}^{[v-1]} - f_u^{[v-1]}}{R_{u+v} - R_u}$$

$$f_u^{[0]} = f(R_u) \qquad (0 \le u \le n, 1 \le v \le n)$$

u and v are integers. $P_n(R)$, $Q_v(R)$, R_u, and $f(R_u)$

are the interpolating polynomial of order n, its v-th product group, the u-th sampling point, and the value of an interpolated function at R_u, respectively. For better understanding, (1), (3) or (4) corresponds to $f(R_u)$, regardless of spectral or spatial domain. Examining (5) and (6), the higher the order of a term in $P_n(R)$ of the DDI becomes, the smaller its coefficient gets, but none of the coefficients can be neglected in the LI case [9]. The procedural averaging (smoothening-out) effect makes the DDI need practically only a few terms of the interpolating polynomial. Whenever a sample is added, the LI calculates all the increased number of terms, but the DDI just adds the new one [9]. However, the DDI with low order interpolating polynomials cannot always guarantee the accuracy in the entire interval of a problem. To overcome this shortcoming of the DDI approach, the spline concept is adopted and SDDI is devised [8]. This means that the entire interval is segmented and different numbers of samples and orders can be determined for interpolation for each interval. In addition, problem-related derivatives can be adopted for spline-realization, considering spatial differentiation.

In applying the SDDI technique to the analysis of a layered media problem, the sampling scheme needs to be carefully chosen. To generate the sampling points, uniformly and non-uniformly spaced sampling schemes can be used. The uniformly spaced sampling scheme is preferred, if R for an impedance matrix element tends to be regularly distributed. Otherwise, the non-uniformly spaced sampling scheme is used.

If an x-directed strip is considered and its length l is much larger than its width w, sampling for interpolation can be made at the points separate by a uniform distance larger than segmentation unit Δx along the x-axis. The distance variable R for the impedance matrix calculation is $k\Delta x$, where k is nonnegative integer varying zero through a number smaller than $l/\Delta x$. So the uniform sampling needs fewer samples than $l/\Delta x$. For the non-uniformly spaced sampling scheme, let Δx and Δy be the unit sizes of basis-function segmentation in x-and y-directions, respectively used for a patch with dimension of $W \times L$. Then, the number of pulse bases necessary in x-direction is $p\ (\equiv W/\Delta x)$ and that in y-direction becomes $q\ (\equiv L/\Delta y)$. R for calculating the impedance matrix elements q corresponds to $\sqrt{m}\times\min(\Delta x, \Delta y)$, where m is nonnegative integer varying zero through $(p-1)^2+(q-1)^2$. Since mutual interactions between the two elements with distance R over four times $\min(\Delta x, \Delta y)$ almost monotonously decrease, the number of R_i is roughly 5 times ($N_{\max}+1$), where $N_{\max}$ is the maximum of n with $P_n(R)$ which can be varied in the segmented interval. For both the two sampling schemes, the value of the interpolated function at a point having distance R is determined by (1) or (4).

III. NUMERICAL RESULTS AND THEIR COMPARISON

In order to show the better performance of the SDDI over the DDI in a given interval, a non-monotonically varying function $f(R)=(R-1.1)(R-2.6)\times(R-3.1)(R-3.9)$ is calculated using both the techniques. In Fig. 1, it is shown that the SDDI with a lower order ($n=3$) produces almost the same values as the DDI with a higher order ($n=5$) gives. This means the SDDI with fewer samples can more efficiently interpolate $f(R)$ than the DDI.

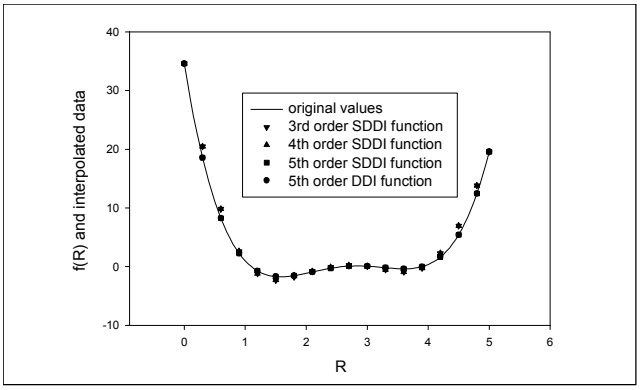

Fig. 1. Comparison of the results obtained by the DDI and the SDDI.

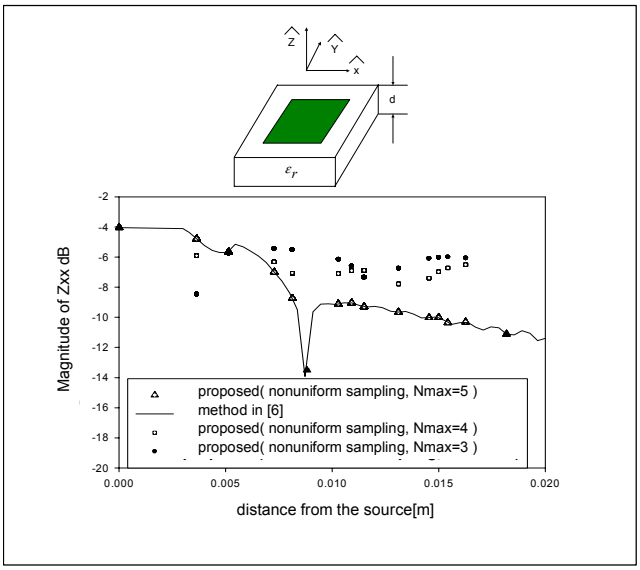

Fig. 2. Magnitude of Z_{xx} as a function of distance from the source point on a microstrip patch with dielectric thickness d = 0.16 cm, relative permittivity ε_r =2.54 , frequency = 2.29 GHz , and $N_{\max}$ =3 – 5.

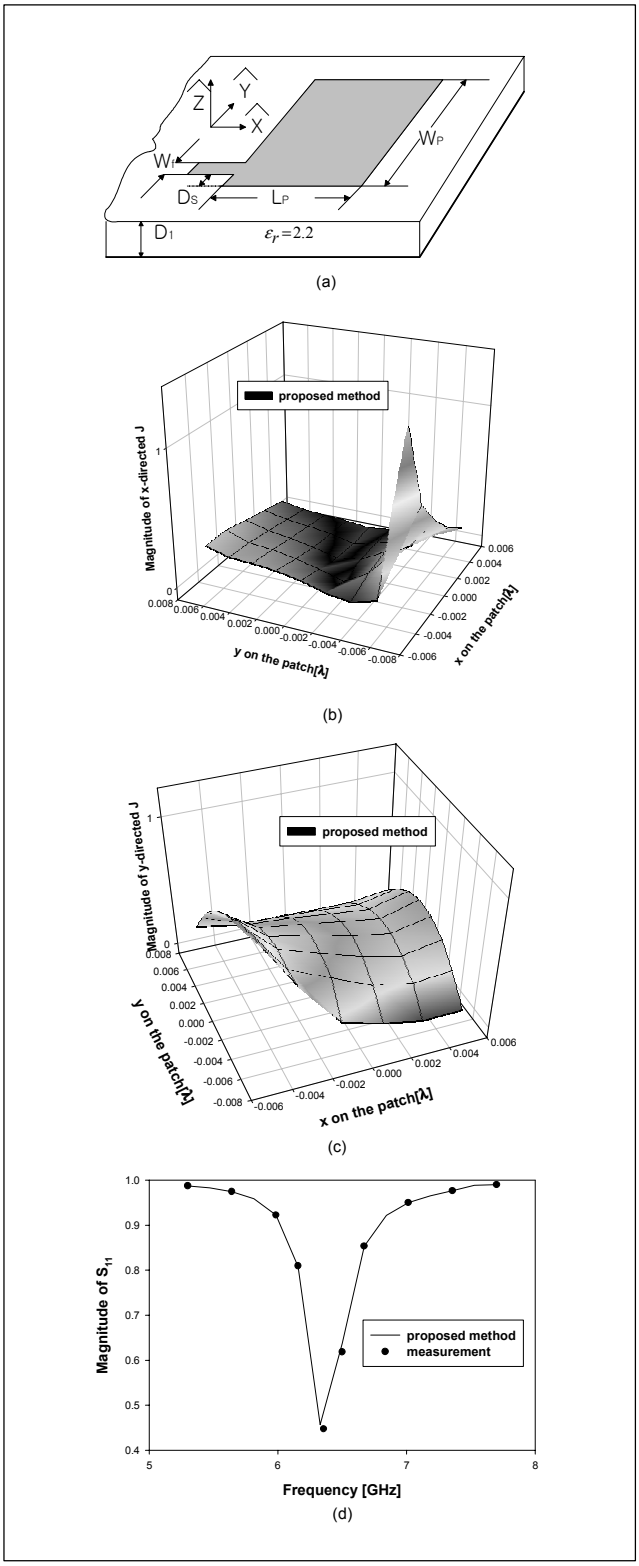

Fig. 3. A line-fed microstrip patch antenna with the same geometrical parameters as those in [10]. (a) 3-D geometry, (b) x-directed current, (c) y-directed current, (d) Magnitudes of S_{11}.

Spectral integrals encountered in analyzing the characteristics of microstrip structures can be calculated by the proposed method. In Fig. 2, the basis-expanded and tested Green's function $Z_{xx}(\vec{\rho}_m - \vec{\rho}_{sn})$ for a 6.25×6.25 cm^2 square patch on a grounded dielectric slab with thickness d = 0.16 cm and relative permittivity ε_r = 2.54 at operating frequency of 2.29 GHz is calculated using the non-uniformly spaced sampling scheme. The segment size is $\Delta x = \Delta y = \lambda/10$ is used for the interpolation. In Fig. 2, the solid line is obtained by the method in [7], and the others represent the results by the proposed method with $N_{\max}$ =3, 4, 5. Z_{xx} is interpolated well for $N_{\max}$ =5, but is not for $N_{\max}$ =3, 4. It indicates that the result starts to converge when $N_{\max}$ is 5.

A line-fed microstrip patch antenna is analyzed by the proposed method for spectral integration, which is more complex than the simple microstrip patch as illustrated in Fig. 2. Geometrical parameters for this structure in Fig. 3(a) are the same as those of [10]. S_{11} is defined as the reflection coefficient at the feeding line. The sampling is non-uniformly performed with n =1 for $0 \le R \le \Delta x$, n =5 for $\Delta x \le R \le 10\Delta x$ and n =1 for $10\Delta x \le R \le 12\Delta x$. The total of used sampling points is 21. Figures 3(b) and 3(c) show the electric surface current densities directed in x- and y- axes, respectively, and they satisfy the edge conditions. S_{11} obtained by the proposed method is in good agreement with that of measurement [10] as is shown in Fig. 3(d).

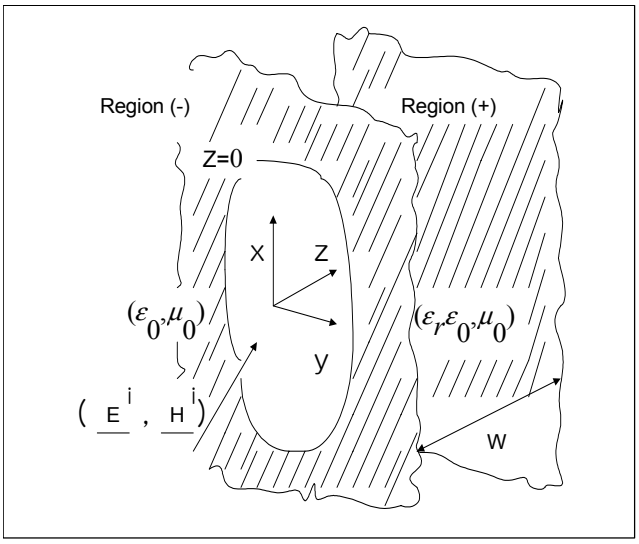

Fig. 4. A parallel plate with an aperture with the same geometrical parameters as those in [11].

Different from the previous problems, when the electromagnetic fields are coupled into the parallel plate through an aperture as in Fig. 4 [11], the summations and derivatives of the Green's function need to be evaluated. Regions $(+)$ $(z > 0)$ and $(-)$ $(z < 0)$ are filled with dielectric materials of $(\varepsilon_r\varepsilon_0, \mu_0)$

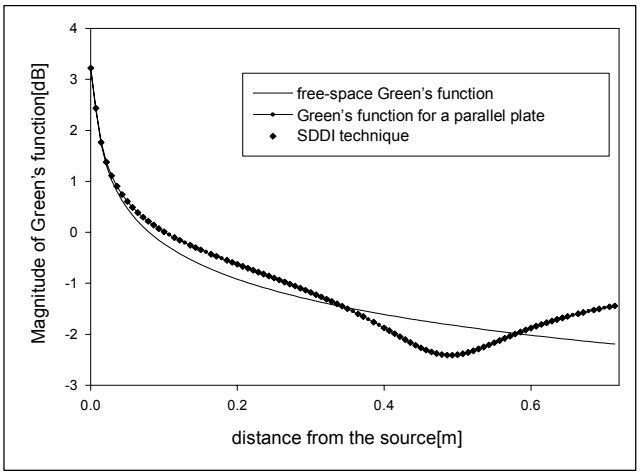

Fig. 5. Comparison of the summation-type Green's function calculated by the SDDI and free-space Green's function.

and (ε_0 , μ_0), respectively. $\varepsilon_r = 1$, and the y-polarized electric field is normally incident on the $0.5\lambda \times 0.5\lambda$ rectangular aperture in an infinite ground plane. The separation between the two plates is 2.8λ. The incident magnetic field is given as

$$\overline{H}^{i,-} = \hat{k}^i \times \hat{y} \frac{e^{-j\overline{k}^i \cdot \overline{r}^i}}{\eta} \tag{7}$$

where $k = \sqrt{\varepsilon_0 \mu_0}$, $\eta = \sqrt{\mu_0 / \varepsilon_0}$, $\overline{k}^i = k_x{}^i \hat{x} + k_y{}^i \hat{y} + k_z{}^i \hat{z}$, $\hat{k}^i = \overline{k}^i / k$ and $\overline{r} = x\hat{x} + y\hat{y} + z\hat{z}$. The summation-type Green's function for the given aperture problem is calculated by the conventional and proposed technique, and the results are compared with free space Green's function in Fig. 5. The truncation number of the summation is set as 300. $P_n(r)$ with $N_{\max} = 5$ is used in the SDDI scheme. In Fig. 5, the values obtained by the SDDI technique (◆) agree very well with those of the summation (-●-). Nine rooftop basis functions are used in x and y directions, respectively, to calculate the magnetic current on the aperture, which is the unknown of the integrodifferential equation. Figure 6 shows the computed distribution of the electric field along x and y directions. The values obtained by the SDDI technique(-) accurately approach those in [11] (●). Figure 6(c) presents that the electric field shows the edge behavior in the y-direction as expected.

To investigate the numerical efficiency of the SDDI technique, the computational time of the proposed method is compared to that of other approach. As shown in Table 1, the proposed technique can save the overall computational times for all these electromagnetic problems. The proposed method with $N_{\max}$ =5 can solve the problem of Fig. 2 about 46% faster than the method in [7]. In the analysis of the line-fed microstrip patch antenna, the computational time is saved by around 47%. For the parallel plate structure, the computational time of 48.76% can be saved by the proposed technique.

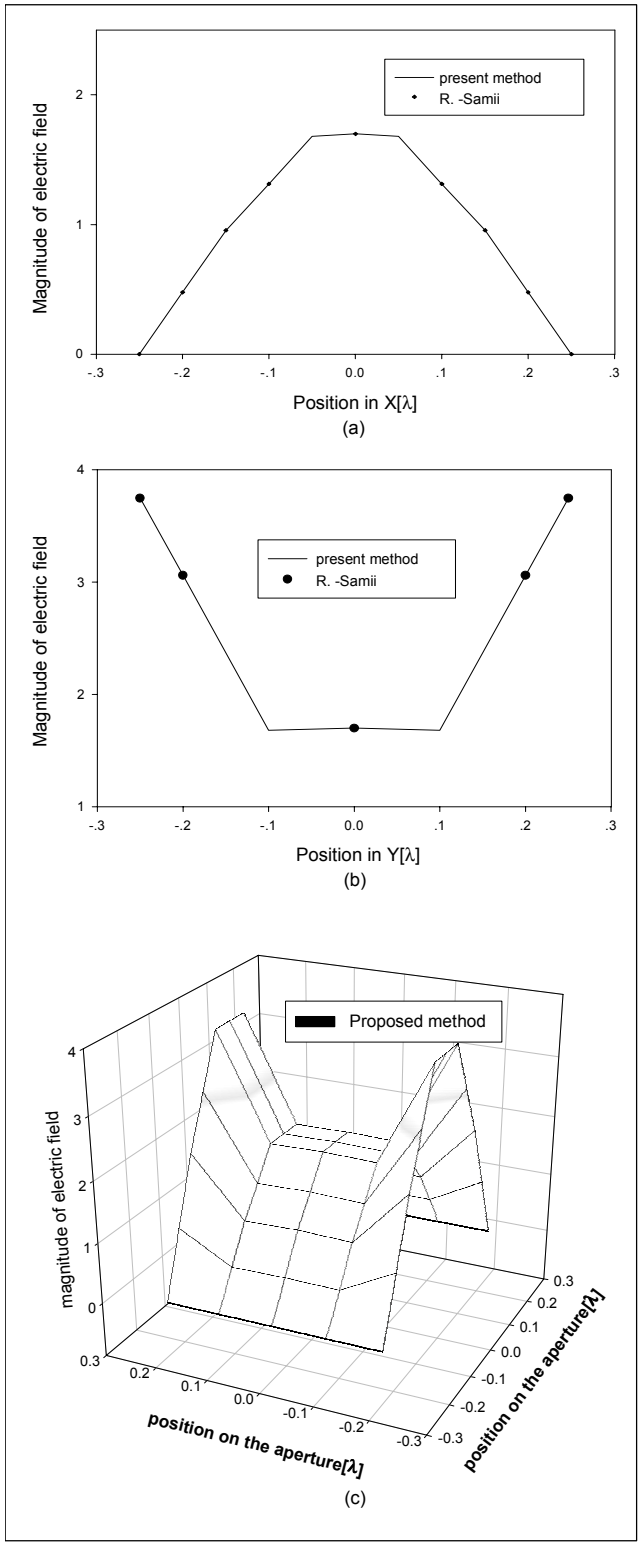

Fig. 6. X-directed electric field distribution on the aperture of the parallel plate. (a) along x-axis, (b) along y-axis, (c) 3-D geometry.

Table 1. Comparison of the computational times.

Problem Structure	Computational times (other methods)		Computational times (proposed method)
Microstrip patch (Fig. 5)	Method in [6]	4.0221×10^3 secs	2.1593×10^3 secs
Line-fed Microstrip patch (Fig. 6)	Method in [6]	4.0688×10^3 secs	2.1603×10^3 secs
Parallel plate structure (Fig. 7)	Direct summation	1.487×10^3 secs	0.762×10^3 secs

IV. CONCLUSION

It is shown that the evaluation of integrodifferential equations including spatial differentiation can be accelerated by the SDDI scheme using fewer samples and spline-concept. Also, the numerical accuracy of the present approach is verified by applying this method to the electromagnetic characterization of a grounded slab and a parallel-plate structure. It is believed that the proposed technique can be extended to solving the electromagnetic equations having highly oscillatory kernels in integral or integrodifferential equations and more complex structures, and it needs to be investigated further in the near future.

REFERENCES

[1] R. W. Jackson and D. M. Pozar, "Full-Wave Analysis of Microstrip Open-End and Gap Discontinuities", *IEEE Trans. Microwave Theory and Tech.*, Vol. 33, Oct. 1985, pp. 1036-1042.

[2] P. L. Sullivan and D. H. Schaubert, "Analysis of an Aperture Coupled Microstrip Antenna", *IEEE Trans. Antennas and Propagat.,* Vol. 34, Feb. 1986, pp. 977-984.

[3] Y. L. Chow *et al.*, "Closed Spatial Green's Function for the Thick Substrate", *IEEE Trans. Microwave Theory and Tech.*, Vol. MTT-39, Mar. 1991, pp. 588-592.

[4] D. G. Fang *et al.*, "Discrete Image Theory for Horizontal Electric Dipoles in a Multilayered Medium", *Proc. IEE*, Vol. 135, Pt. Oct. 1991.

[5] J. W. Ko, "Scattering from a Periodic Array of Double-Dipole Elements over Grounded Dielectric Slab", *ETRI Journal*, Vol. 20, No. 1, Mar. 1998.

[6] T. Itoh, *Numerical Techniques For Microwave and Millimeter-wave Passive Structures*, John Wiley & Sons, New York, 1989.

[7] S.-O. Park and C. A. Balanis, "Analytical Evaluation of the Asymptotic Impedance Matrix of a Grounded Dielectric Slab with Roof-Top Functions", *IEEE Trans. Antennas and Propagat.*, Vol. 46, Feb. 1998, pp. 251-259.

[8] S. Kahng and J. Choi, "An Efficient Impedance Matrix Calculation using the Spline-type Divided Difference Interpolation Technique", *IEEE, Microwave and Guided Wave Letters*, Vol. 9, No. 7, July 1999, pp. 268 – 270.

[9] C. F. Gerald *et al.*, *Applied Numerical Analysis*, Addison Wesley, New York, 1994.

[10] I. J. Bahl and P. Bhartia, *Microstrip Antennas*, Artech House, Dedham, Massachusetts, 1980.

[11] Y. Rahmat-Samii, "Electromagnetic Coupling into the Parallel Plate through Apertures", *IEEE Trans. Electromagnetic Compatibility*, Vol. EMC-20, No. 3, Aug. 1978, pp. 436 –442.

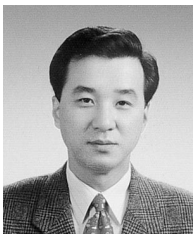

Jaehoon Choi received the B.S. degree in electronics engineering from Hanyang University, Seoul, Korea in 1980, the M.S. and Ph.D degrees in electrical engineering in 1986 and 1989, respectively, both from the Ohio State University. From 1989 to 1991, he was with the Telecommunications Research Center at Arizona State University, as a research scientist. In 1991, he joined the Korea Telecom, Seoul, Korea, where he was engaged in the research and development of Koreasat payload system. Since1995, he has been with Hanyang University as an assistant professor in the division of electrical and computer engineering. His research interests include mobile and satellite communication antenna design and analysis, fullwave analysis of passive devices, propagation modeling and interference analysis of mobile and satellite communication systems, and EMC analysis of a high speed digital circuit. He has published over 25 technical papers throughout the major international journals and conferences.

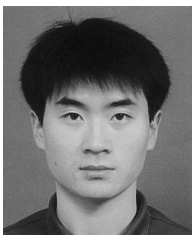

Sungtek Kahng received the Ph.D. degree of electronics from Hanyang University, Seoul, Korea in 2000, with the field of specialty in radio science and engineering. From 1996 to 2000, he held the positions of the primary research assistant and researcher at the Institute of Science and Technology of the same university, where he mainly conducted research on computational electromagnetics and its development and application. Since 2000, he has been working for the Electronics and Telecommunications Research Institute, Taejon, Korea. He is included in research, design and development of passive devices for satellites and has much interest in research on numerical modeling, analysis, electromagnetic characterization of RF devices and circuits.